www.MaterialsViews.com

Carbon Nanotubes

# Strong and Conductive Dry Carbon Nanotube Films by Microcombing

*Liwen Zhang, Xin Wang, Weizong Xu, Yongyi Zhang, Qingwen Li, Philip D. Bradford, and Yuntian Zhu**

*In order to maximize the carbon nanotube (CNT) buckypaper properties, it is critical to improve their alignment and reduce their waviness. In this paper, a novel approach, microcombing, is reported to fabricate aligned CNT films with a uniform structure. High level of nanotube alignment and straightness was achieved using sharp surgical blades with microsized features at the blade edges to comb single layer of CNT sheet. These microcombs also reduced structural defects within the film and enhanced the nanotube packing density. Following the microcombing approach, the as-produced CNT films demonstrated a tensile strength of up to 3.2 GPa, Young's modulus of up to 172 GPa, and electrical conductivity of up to $1.8 \times 10^5$ S $m^{-1}$, which are much superior to previously reported CNT films or buckypapers. More importantly, this novel technique requires less rigorous process control and can construct CNT films with reproducible properties.*

## 1. Introduction

Carbon nanotubes (CNTs), with superior mechanical properties, high thermal, and electrical conductivities, have been the focus of extensive research for structural composites,[1,2] thermal interface materials,[3–5] and electrical conductors.[6–8] Researchers have devoted great effort to exploring high strength and lightweight CNT reinforcements for composites, by designing novel structures of CNT assemblies at the micro- and nano-scales.[9–14] CNTs, as reinforcements for composites, have been developed in the forms of fibers and films (also named buckypapers, sheets, where buckypaper often specifically refers to randomly oriented CNT paper). Among these, CNT films and buckypapers have drawn increasing interest due to their outstanding 2D or 3D properties, easy fabrication, and amenability for scaled-up production.

In solution-based or melt-processing fabrication of CNT films and buckypapers, the large surface area and high aspect ratio of CNTs make them extremely difficult to disperse in solution or melt, and thus gives rise to nonuniform structures.[14] Short CNTs (<10 μm), although easier to disperse, usually render inefficient load transfer across the weakly bonded interfaces in resultant composites,[11] as the short nanotubes are only held by weak van der Waals forces. Consequently, the mechanical properties of CNT buckypapers produced by short-CNT dispersion have very low strengths of only about 10 MPa and low Young's moduli of less than 1 GPa.[15–20] These are far below the properties of individual CNTs and would limit their potential for envisioned applications. Many attempts have been made to improve the mechanical and electrical properties of buckypapers through promoting nanotube dispersion[16,17,21,22] or increasing intertube bonding to construct a 2D or 3D CNT network within the buckypaper.[18,23] However, no significant progress has been made in achieving the predicted properties.

L. W. Zhang, Dr. X. Wang, Dr. W. Z. Xu, Prof. Y. T. Zhu
Department of Materials Science and Engineering
North Carolina State University
NC 27695, USA
E-mail: ytzhu@ncsu.edu

Dr. Y. Y. Zhang, Prof. Q. W. Li
Suzhou Institute of Nano-Science and Nano-Biotics
Suzhou 215123, China

Prof. P. D. Bradford
College of Textile
North Carolina State University
NC 27695, USA

DOI: 10.1002/smll.201500111

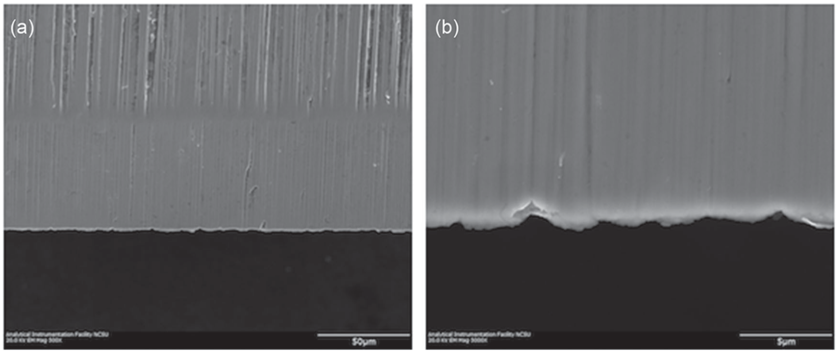


Figure 1. Microfeatures of the edge of the microcombing blade.

Recently, it has been found that the CNT alignment has a profound impact on the mechanical and electrical properties of CNT films and buckypapers.[20,24–27] “Domino pushing” and “shear pressing” approaches have been developed to fabricate aligned CNT buckypapers directly from vertically aligned CNT arrays.[24,26] The long and aligned CNTs have effective contacts against each other along their alignment direction, and thus contributing to efficient load and electron transfer. However, the size of the as-produced buckpaper is usually limited by the size of the array substrate because of the nature of “domino pushing” and “shear pressing” approaches. In another work, CNT buckypapers produced by the floating catalyst chemical vapor deposition (FCCVD) method were processed by a stretching–pressing approach and resulted in a high degree of CNT alignment and thus increased the tensile strength by 200%[27] compared with the nonstretched ones.[28,29] In 2002, Fan and co-workers developed drawable CNTs, which allow a vertically super-aligned CNT array to convert into a horizontally aligned 2D CNT sheet.[10] Rather than the 3D CNT array, this 2D CNT sheet has a high degree of CNT alignment in the horizontal direction, which maximizes the potentials of the CNTs while constructing them into multiple forms, such as CNT yarns and layered CNT films. Inoue et al. took advantage of this drawable feature of the super-aligned CNTs, used a winding method to fabricate anisotropic CNT films from multi-walled CNT arrays, and achieved a tensile strength of 75.6 MPa and an electrical conductivity of $4 \times 10^4$ S $m^{-1}$.[30] In 2012, Di et al. used few-walled CNT arrays to produce aligned CNT films by a similar winding method coupled with ethanol-densification, and achieved a tensile strength up to 2 GPa and Young’s modulus up to 90 GPa.[31] More recently, they renewed their record to 2.96 and 124 GPa for the tensile strength and Young’s modulus by densification using ethanol and acetone, respectively.[32]

Apart from CNT alignment, another critical issue that limits the CNT film property is CNT waviness, as pointed out in our previous work.[33,34] In approaches of fabricating CNT/Polymer composite films, stretching was proved effective in reducing CNT waviness and improving composite properties. However, stretching of a single layer of aligned CNT sheet is extremely difficult. It requires exceptionally careful control of stretching rate and very high quality of drawable CNT arrays.

In this work, we present a simple and effective approach, called “microcombing”, to reduce CNT waviness directly at their single-layer level before the potential formation of large CNT bundles. Principally based on the previously reported winding technique, this method, for the first time, utilizes a micro-scale rough surface to locally mitigate entangled bundles and straighten the wavy CNTs. The as-combed single layer of CNT sheet exhibits high level of nanotube alignment and straightness, which leads to a uniform structure of CNT film with a tensile strength of up to 3.2 GPa, Young’s modulus of up to 172 GPa, and electrical conductivity of up to $1.8 \times 10^5$ S $m^{-1}$. More importantly, the microcombing approach is not restricted to high quality of drawable arrays, requires less rigorous process control, and can construct CNT films with reproducible properties.

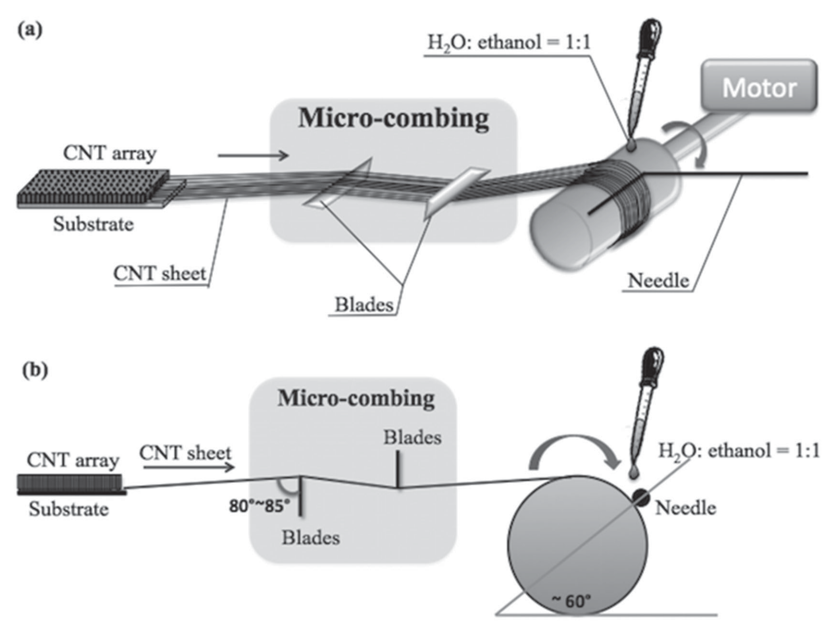


Figure 2. Microcombing process: a) schematic overview; b) schematic side view.

## 2. Experimental Section

*Materials*: The drawable CNT arrays used in the experiment were synthesized using a chemical vapor deposition method.[31] The CNT arrays were approximately 200 μm in height, with individual nanotubes having 2–5 walls and 5–7 nm in diameters.

*Microcombing Process*: The key component of the process, microcombing of individual layer of CNT sheets, is accomplished by using two oppositely positioned

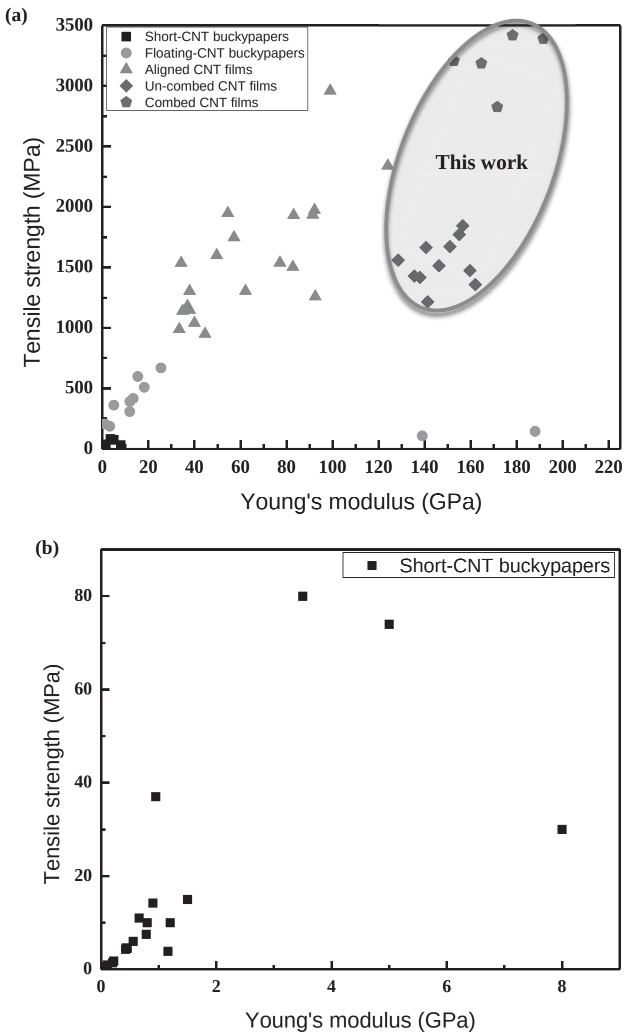


Figure 3. Mechanical properties of CNT films: a) comparison of combed CNT films with previously reported buckypapers and other aligned CNT films; b) enlargement of the data area for buckypapers produced by short CNT dispersion.

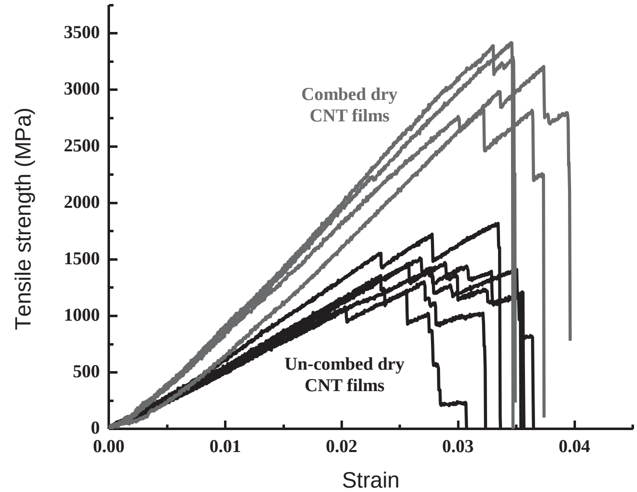


Figure 4. Typical tensile stress–strain curves of the uncombed and combed dry CNT films.

surgical blades. Scanning electron microscopy (SEM) images (**Figure 1**) of the blade edge show microfeatures (teeth width: ≈2 μm, teeth depth: ≈0.5 μm), which can act as microcombs to disentangle and straighten the wavy CNTs.

The experimental setup is shown by the schematics in **Figure 2**, when a layer of CNT sheet was drawn out from the CNT array, it passed two surgical blades, then wound to a rotating mandrel with a diameter of 3 cm at a speed of 20 r min$^{-1}$. The contact angle between the CNT sheet and the blade was controlled at 80°–85°. A metal needle with a diameter of 0.65 mm bent into 90° was placed on the mandrel at 1 o'clock position, coating the densifying solution on the CNT sheet layer by layer during the winding process, as shown in Figure 2b. The densifying solution consists of deionized water and ethanol with a mixing ratio of 1:1 by volume.

200 revolutions produced a film with a thickness of about 3 μm. The CNT film was then peeled off from the mandrel and hot-pressed at 80 °C for 2 h under a pressure of 10 MPa. Under high pressure, the film was condensed to about 2 μm. Since the coating solution was $H_2O$ and ethanol, they evaporated during the process, leaving a pure dry CNT film with aligned long CNTs.

*Characterization Methods*: Tensile test specimens were cut from both the uncombed and combed dry CNT films. The test coupons are typically 1-mm wide and a gauge length of 10 mm. The width was measured using a calibrated scale bar in an optical micrometer. The sample thickness was measured by a micrometer and further confirmed by SEM (HITACHI S-4800). Tensile tests were conducted using an Instron 3365 tensile testing machine with a load cell of 10 N and a strain rate of 0.5 mm min$^{-1}$. The weight of each specimen was measured at University of Delaware using a MX5 microbalance by Mettler-Toledo, Inc., which had an accuracy of 1 mg. Specimen density was calculated based on the measured dimension and weight. Surface morphology of both the combing blades and the as-produced dry films were analyzed by SEM (Verio 460L) and transmission electron microscope (TEM, Tecnai G2 F20 S-TWIN). A 4-probe Agilent 34410A 6.5 digit multimeter was used to test the electrical conductivity of the films along the CNT direction. Silver electrodes were produced by magnetron sputtering.

## 3. Results and Discussion

### 3.1. Mechanical Properties

**Table 1** and **Figure 3** compare the mechanical properties of the dry CNT films produced by microcombing with previously reported data. The CNT buckypapers made of short CNTs are named as short-CNT buckypapers; the buckypapers produced by FCCVD method are called floating-CNT buckypapers; and the CNT films made by winding 2D CNT sheet from the drawable arrays are called aligned CNT films. The tensile strength of the as-produced uncombed dry CNT films of (1.56 ± 0.19) GPa agrees well with the previously reported data for aligned CNT films (1.0–2.0 GPa). By microcombing, the tensile strength of the CNT film was

**Table 1.** Mechanical property comparison for buckypapers and dry CNT films.

| Type | Material | Treatment | Young's modulus [GPa] | Tensile strength [MPa] | Ref. |
|---|---|---|---|---|---|
| Short-CNT buckypapers | SWCNT | | 1.2 | 10 | [15] |
| | SWCNT | | 0.8 | 10 | [16] |
| | | $HNO_3$ | 5 | 74 | |
| | SWCNT | | 0.66 | 11 | [17] |
| | | $SOCl_2$ | 0.95 | 37 | |
| | SWCNT | | 1.5 | 6–15 | [18] |
| | | Irradiation | 3.5 | 80 | |
| | MWCNT | | 0.4–0.8 | 4.3–7.5 | [19] |
| | SWCNT | | 0.9 | 14.2 | [20] |
| | SWCNT | Oleum + heat | 8 | 30 | [21] |
| | MWCNT | Chemicals | 0.08–1.16 | 0.42–3.88 | [22] |
| Floating-CNT buckypapers | MWCNT | | 1.10 | 205 | [25] |
| | | 30% stretch | 11.93 | 390 | |
| | | 35% stretch | 18.21 | 508 | |
| | | 40% stretch | 25.45 | 668 | |
| | Few-walled CNT | | 3.2 ± 0.5 | 186 ± 19 | [27] |
| | | Stretch | 11.9 ± 0.6 | 307 ± 28 | |
| | | Stretch+press once | 13.4 ± 0.5 | 416 ± 25 | |
| | | Stretch+press twice | 15.4 ± 1.0 | 598 ± 36 | |
| | SWCNT | | 188 | 144 | [28] |
| | | Purification | 139 | 107 | |
| | SWCNT | | 5 | 360 | [29] |
| Aligned CNT films | Few-walled CNT | | 33.4–92.5 | 950–1973 | [31] |
| | Few-walled CNT | | 40 ± 5 | 1.04 ± 0.07 (GPa) | [32] |
| | | Ethanol-densified | 124 ± 14 | 2.34 ± 0.31 (GPa) | |
| | | Acetone-densified | 99 ± 11 | 2.96 ± 0.29 (GPa) | |
| | Few-walled CNT | Uncombed | 151 ± 18 | 1561 ± 188 | This work |
| | | Combed | 172 ± 13 | 3206 ± 212 | |

**Table 2.** Electrical conductivity values of the CNT films produced in our work and the data from the literatures.

| Type | Material | Treatment | Electrical conductivity [S m$^{-1}$] | Ref. |
|---|---|---|---|---|
| Short-CNT buckypapers | SWCNT | | $3 \times 10^4$ | [16] |
| | | $HNO_3$ | $1.2 \times 10^4$ | |
| | SWCNT | | $7 \times 10^4$ | [17] |
| | | $SOCl_2$ | $3.5 \times 10^5$ | |
| | MWCNT | | $0.83 \times 10^4$ to $1.0 \times 10^4$ | [19] |
| | SWCNT | Oleum | $1.3 \times 10^5$ | [21] |
| | | Oleum + heat | $9 \times 10^4$ | |
| | MWCNT | Chemicals | $6.53 \times 10^2$ to $18.18 \times 10^2$ | [22] |
| | MWCNT | | $1.5 \times 10^4$ | [24] |
| | | Oriented | $2 \times 10^4$ | |
| Floating-CNT buckypapers | MWCNT | | $4.2 \times 10^4$ | [25] |
| | | 40% stretch | $6.0 \times 10^4$ | |
| | SWCNT | | $2 \times 10^5$ | [29] |
| Aligned CNT films | MWCNT | | $4 \times 10^4$ | [30] |
| | Few-walled CNT | | $3.5 \times 10^4$ | [31] |
| | Few-walled CNT | | $1.16 \times 10^4$ | [32] |
| | | Ethanol-densified | $3.18 \times 10^4$ | |
| | | Acetone-densified | $3.49 \times 10^4$ | |
| | Few-walled CNT | Uncombed | $1.0 \times 10^5 \pm 1156$ | This work |
| | | Combed | $1.8 \times 10^5 \pm 21173$ | |

  

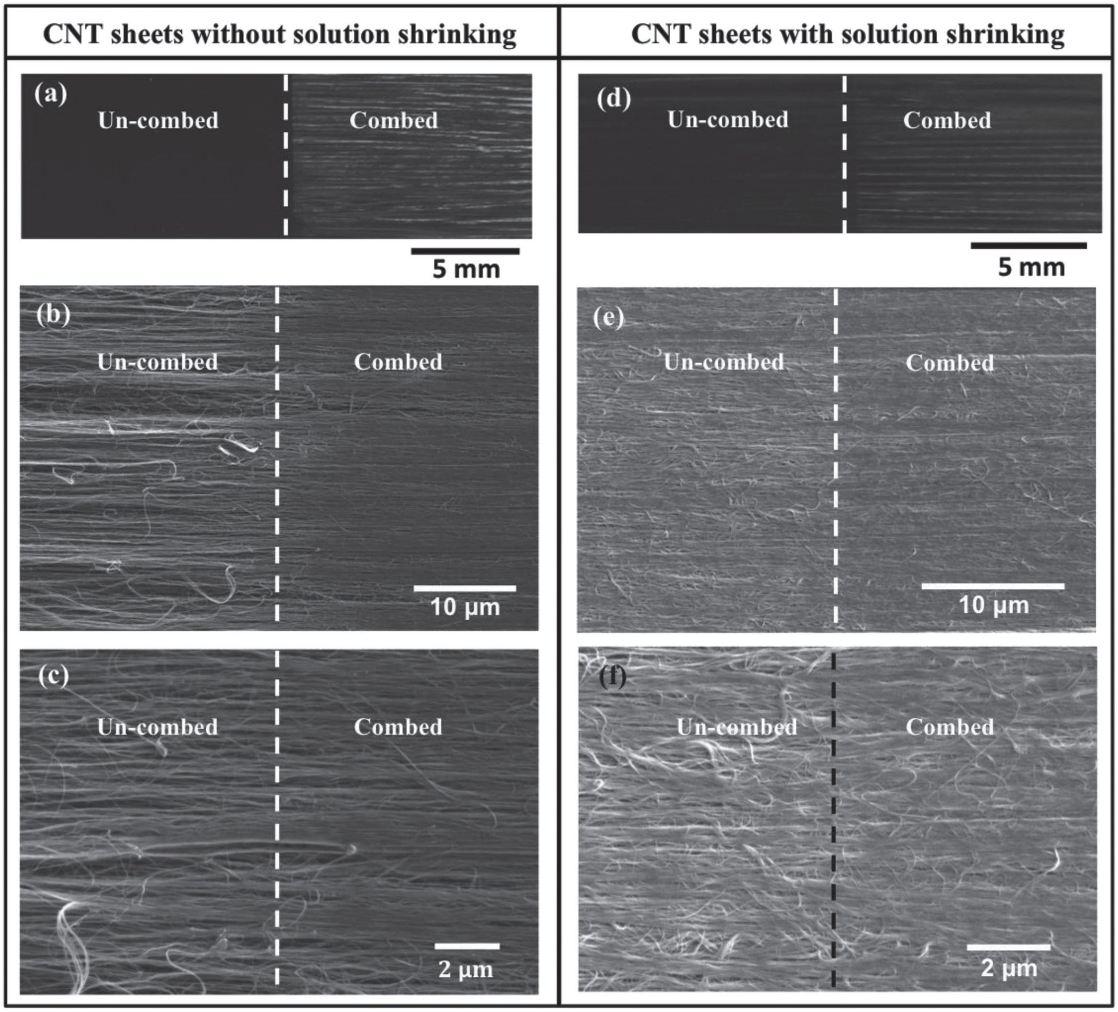


**Figure 5.** a,d) Optical photos and b,c,e,f) SEM images showing the differences between the uncombed and combed dry CNT sheets.

improved by 105% from (1.56 ± 0.19) GPa to (3.21 ± 0.21) GPa, which surpasses the mechanical properties of CNT films or buckypapers reported earlier. Also, the Young's modulus has a ≈14% increase to (172 ± 13) GPa compared with the uncombed films. The density of the uncombed dry films is 0.84 g $cm^{-3}$, whereas the density of the combed dry films is 1.04 g $cm^{-3}$. Thus, the specific tensile strength of the combed dry CNT films is calculated to be 3.08 GPa g $cm^{-3}$. The higher density of the combed dry CNT films indicates enhanced nanotube packing resulted from microcombing. In comparison, the reported density of the aligned CNT films is typically 0.9 g $cm^{-3}$,[31] which is lower than our combed films. With a higher packing density, the aligned CNTs have a stronger inter-tube interaction, which in turn results in a more effective load transfer in the structure.

**Figure 4** displays typical tensile stress–strain curves for the uncombed and combed dry CNT films. The slopes of the combed films show an apparent change compared with the uncombed ones. The Young's modulus is significantly improved by the microcombing. This is a direct evidence of the reduction of the CNT waviness and the improvement in the CNT alignment. In addition, the combed CNT films exhibit a higher tensile strain than that of the uncombed films, suggesting a reduction of structural defects induced by microcombing. The microcombing is simple, effective, and does not require a narrow window of controlled parameters, which greatly promotes the reproducibility and repeatability of the film properties.

### 3.2. Electrical Properties

**Table 2** compares the electrical conductivity of the combed-CNT films and other CNT buckypaprs and films. In our work, the uncombed CNT films exhibit a high electrical conductivity of $1.0 \times 10^5$ S $m^{-1}$, which is among the highest reported values. After microcombing, the electrical conductivity is further improved by 80% to $1.8 \times 10^5$ S $m^{-1}$. This substantial increase in electrical conductivity is also a direct result from better inter-tube contact to facilitate electron transfer due to the improved CNT straightness, enhanced CNT alignment, and higher nanotube packing density.

### 3.3. Effect of Microcombing on the CNT Structure

Combing, which has been used for centuries in the textile industry, is a process to disentangle and straighten staple fibers in order to achieve higher level of fiber alignment in the fiber web.[35] In this work, sharp surgical blades with microscale features at the blade edges were used to disentangle and straighten the wavy CNTs in the as-drawn CNT sheet. One pair of the blades was used to comb both the top-side and bottom-side of the CNT sheet, giving a uniform microcombing (Figure 2). Coming with more blades was found to break CNT sheets or to group CNTs into nonuniform bundles, which is not desired. Additionally, the rotating speed and the contact angle between the CNT sheet and the combing blades are important. It was found fast drawing/rotating speed of the CNT sheet could benefit the CNT alignment. But when the speed was too fast, weak van der Waals forces could not hold the CNTs together any more, leading to the breakage of the CNT sheet. 20 r $min^{-1}$ was the fastest speed that we found to operate successfully. In our experiment, the contact angle between the CNT sheet and the combing blades was controlled at 80°–85° (Figure 2b), which was the optimum angle that we found to allow CNT sheet to be fully combed without breakage. When using smaller contact angles (less than 80°–85°), the contact surface between the CNT sheet and the blade became larger. The increased friction made the nanotubes accumulate onto the edge of the blade, and break the CNT sheet at the blade. When using larger contact angles, the effect of microcombing was less effective in improving the packing and alignment of CNTs.

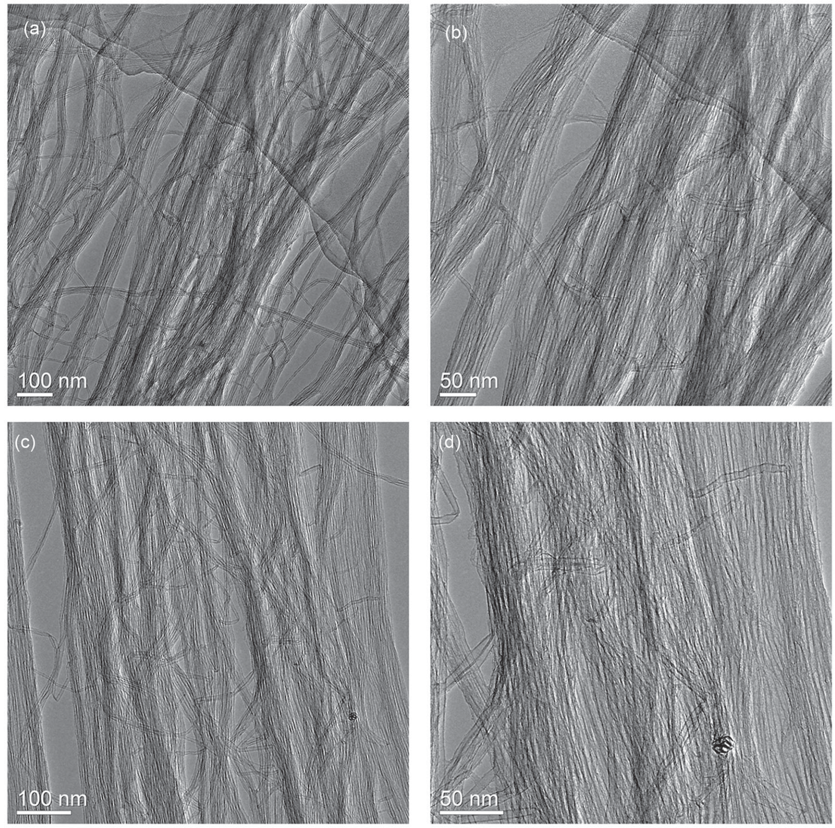

Figure 6. TEM images of one single layer of CNT sheet a,b) before and c,d) after microcombing.

**Figure 5** shows both the optical photos and SEM images of the dry CNT sheets before and after microcombing, and before and after solution treatment, respectively. After the microcombing process, it is evident that the CNT sheets become shiny due to their smoothened surfaces (Figure 5a,b). As shown in the SEM images (Figure 5b,c,e,f), the microcombing process reduced the waviness of CNTs and enhanced the structural uniformity. This is also demonstrated by the TEM images of a single layer of CNT sheet before and after microcombing, as shown in **Figure 6**. After solution treatment (Figure 5e,f), the nanotubes formed larger bundles and the sheets became denser. This was caused by the shrinking and densification effect of the ethanol in the coating solution.

## 4. Conclusion

A novel "microcombing" approach is developed in this study to fabricate dry CNT films with ultrahigh mechanical properties and exceptional electrical performances. The approach has been shown to be effective in mitigating CNT waviness, reducing film defects, and improving CNT alignment and packing. The dry CNT films produced by microcombing exhibited very high Young's modulus of 172 GPa, excellent tensile strength of 3.2 GPa, and unprecedented electrical conductivity of $1.8 \times 10^5$ S $m^{-1}$. This approach is simple and effective, and can greatly improve the reproducibility and repeatability of the CNT film properties.

## Acknowledgements

*The authors are grateful to Suzhou Institute of Nano-Science and Nano-Biotics for providing the CNT arrays. The authors also thank Jiali Yu, a student in the University of Delaware, for her help with the sample weight measurement. This work was funded by the US Air Force Office of Scientific Research (Grant No. FA9550–12–1–0088).*

[1] L. Wei, X. H. Zhang, G. Xu, P. D. Bradford, X. Wang, H. B. Zhao, Y. Y. Zhang, Q. X. Jia, F. G. Yuan, Q. W. Li, Y. P. Qiu, Y. T. Zhu, *Carbon* **2011**, *49*, 4786.
[2] X. F. Zhang, Q. W. Li, T. G. Holesinger, P. N. Arendt, J. Y. Huang, P. D. Kirven, T. G. Clapp, R. F. DePaula, X. Z. Liao, Y. H. Zhao, L. X. Zheng, D. E. Perterson, Y. T. Zhu, *Adv. Mater.* **2007**, *19*, 4198.
[3] R. S. Ruoff, D. C. Lorents, *Carbon* **1995**, *33*(7), 925–30.

[4] M. J. Biercuk, M. C. Llaguno, M. Radosavljevic, J. K. Hyun, A. T. Johnson, J. E. Fischer, *Appl. Phys. Lett.* **2002**, *75*(15), 2767–2769.
[5] J. Wang, J. S. Wang. *Appl. Phys. Lett.* **2006**, *75*(11), 111909.
[6] C. Niu, E. K. Sichel, R. Hoch, D. Moy, H. Tennent, *Appl. Phys. Lett.* **1997**, *75*(11),1480–1482.
[7] K. H. An, W. S. Kim, Y. S. Park, Y. C. Choi, S. M. Lee, D. C. Chung, D. J. Bae, S. C. Lim, Y. H. Lee, *Adv. Mater.* **2001**, *13*(7), 497–500.
[8] S. Rosenblatt, Y. Yaish, J. Park, J. Gore, V. Sazonova, P. L. McEuen, *Nano Lett.* **2002**, *2*(8), 869–8672.
[9] E. T. Thostenson, Z. Ren, T. Chou, *Composites Sci. Technol.* **2001**, *61*(13), 1899–912.
[10] K. L. Jiang, Q. Q. Li, S. S. Fan, *Nature* **2002**, *419*(6909), 801.
[11] P. M. Ajayan, T. M. James, *Nature* **2007**, *447*(7148), 1066–1068.
[12] H. D. Wagner, *Nature Nanotechnol.* **2007**, *2*(12), 742–744.
[13] W. J. Ma, L. Q. Liu, Z. Zhang, R. Yang, G. Liu, T. H. Zhang, X. F. An, X. S. Yi, Y. Ren, Z. Q. Niu, J. Z. Li, H. B. Dong, W. Y. Zhou, P. M. Ajayan, S. S. Xie, *Nano Lett.* **2009**, *9*(8), 2855.
[14] J. T. Di, X. Wang, Y. Y. Xing, Y. Y. Zhang, X. H. Zhang, W. B. Lu, Q. W. Li, Y. T. Zhu, *Small* **2014**, *10*(22), 4606–4625.
[15] R. H. Baughman, C. Cui, A. A. Zakhidov, Z. Iqbal, J. N. Barisci, G. M. Spinks, G. G. Wallace, A. Mazzoldi, D. D. Rossi, A. G. Rinzler, O. Jaschinski, S. Roth, M. Kertesz, *Science* **1999**, *284*(5418), 1340–1344.
[16] X. F. Zhang, T. V. Sreekumar, T. Liu, S. Kumar. *J. Phys. Chem. B* **2004**, *108*(42), 16435–16440.
[17] U. Dettlaff-Weglikowska, D. Tománek, S. Roth, V. Skákalová, R. Graupner, S. H. Jhang, B. H. Kim, H. J. Lee, L. Ley, Y. W. Park, *J. Am. Chem. Soc.* **2005**, *127*(14), 5125.
[18] S. R. Wang, Z. Y. Liang, B. Wang, C. Zhang, *Adv. Mater.* **2007**, *19*(9), 1257–1261.
[19] G. H. Xu, Q. Zhang, W. P. Zhou, J. Q. Huang, F. Wei, *Appl. Phys. A* **2008**, *92*(3), 531–539.
[20] J. G. Park, J. Smithyman, C. Y. Lin, A. Cooke, A. W. Kismarahardja, S. Li, R. Liang, J. S. Brooks, C. Zhang, B. Wang, *J. Appl. Phys.* **2009**, *106*(10), 104310.
[21] T. V. Sreekumar, T. Liu, S. Kumar, L. M. Ericson, R. H. Hauge, R. E. Smalley, *Chem. Mater.* **2003**, *15*(1), 175–178.
[22] Z. Špitalský, C. Galiotis, C. Aggelopoulos, G. Tsoukleri, C. Tsakiroglou, J. Parthenios, S. Georga, C. Krontiras, D. Tasis, K. Papagelis, *Mater. Sci. Eng. B* **2009**, *165*(3), 135–138.
[23] A. Kis, G. Csanyi, J. P. Salvetat, T. N. Lee, E. Couteau, A. J. Kulik, W. Benoit, J. Brugger, L. Forro, *Nat. Mater.* **2004**, *3*(3), 153–157.
[24] D. Wang, P. C. Song, C. H. Liu, W. Wu, S. S. Fan, *Nanotechnology* **2008**, *19*(7), 075609.
[25] Q. F. Cheng, J. W. Bao, J. Park, Z. Y. Liang, C. Zhang, B. Wang, *Adv. Funct. Mater.* **2009**, *19*(20), 3219–3225.
[26] P. D. Bradford, X. Wang, H. B. Zhao, J. P. Maria, Q. X. Jia, Y. T. Zhu, *Composites Sci. Technol.* **2010**, *70*(13), 1980–1985.
[27] Q. L. Liu, M. Li, Y. Z. Gu, Y. Y. Zhang, S. K. Wang, Q. W. Li, Z. G. Zhang, *Nanoscale* **2014**, *6*(8), 4338–4344.
[28] L. Song, L. Ci, L. Lv, Z. P. Zhou, X. Q. Yan, D. F. Liu, H. J. Yuan, Y. Gao, J. X. Wang, L. F. Liu, X. W. Zhao, Z. X. Zhang, X. Y. Dou, W. Y. Zhou, G. Wang, C. Y. Wang, S. S. Xie, *Adv. Mater.* **2004**, *16*(17), 1529–1534.
[29] W. J. Ma, L. Song, R. Yang, T. H. Zhang, Y. C. Zhao, L. F. Sun, Y. Ren, D. F. Liu, L. F. Liu, J. Shen, Z. X. Zhang, Y. J. Xiang, W. Y. Zhou, S. S. Xie, *Nano Lett.* **2007**, *7*(8), 2307–2311.
[30] Y. Inoue, Y. Suzuki, Y. Minami, J. Muramatsu, Y. Shimamura, K. Suzuki, A. Ghemes, M. Okada, S. Sakakibara, H. Mimura, K. Naito, *Carbon* **2011**, *49*(7), 2437–2443.
[31] J. T. Di, D. M. Hu, H. Y. Chen, Z. Z. Yong, M. H. Chen, Z. H. Feng, Y. T. Zhu, Q. W. Li, *ACS Nano* **2012**, *6*(6), 5457–5464.
[32] Y. J. Wang, M. Li, Y. Z. Gu, X. H. Zhang, S. K. Wang, Q. W. Li, Z. G. Zhang, *Nanoscale* **2015**, *7*(7), 3060–3066.
[33] X. Wang, P. D. Bradford, W. Liu, H. B. Zhao, Y. Inoue, J. P. Maria, Q. W. Li, F. G. Yuan, Y. T. Zhu, *Composites Sci. Technol.* **2011**, *71*(14), 1677–1683.
[34] X. Wang, Y. T. Zhu, Z. Z. Yong, Q. W. Li, P. D. Bradford, W. Liu, D. S. Tucker, W. Cai, H. Wang, F. G. Yuan, *Mater. Res. Lett.* **2013**, *1*(1), 19–25.
[35] C. A. Lawrence, *Scitech. Book News* **2003**, *27*, 238.

Received: January 14, 2015
Revised: March 10, 2015
Published online: May 4, 2015